PALEONTOLOGY

An additional brain endocast of the ictidosaur *Riograndia guaibensis* (Eucynodontia: Probainognathia): intraspecific variation of endocranial traits

LEONARDO KERBER, JOSÉ D. FERREIRA, PEDRO HENRIQUE M. FONSECA, ARYMATHEIA FRANCO, AGUSTÍN G. MARTINELLI, MARINA B. SOARES & ANA MARIA RIBEIRO

Abstract: Recently, the morphology and encephalization of the brain endocast of the Triassic non-mammaliaform probainognathian cynodont *Riograndia guaibensis* were studied. Here, we analyzed the brain endocast of an additional specimen of this species. The new endocast shows well-defined olfactory bulbs and a median sulcus dividing the hemispheres, traits that were not clearly observed in the first studied specimen. Encephalization quotients were also calculated, revealing similar values to other non-mammaliaform cynodonts and lower than those of the first analyzed specimen. The analyzed cranium is slightly larger than the first studied one and may represent an advanced ontogenetic stage. Hence, these differences may be related to the intraspecific variation of this cynodont or alternatively, to the preservation of each specimen.

Key words: Endocranium, Ictidosauria, Micro-CT, paleoneurology.

INTRODUCTION

With the advance of the CT-Scanning techniques, the endocranial study of therapsids has been significantly increased in the last years (*e.g.*, Castanhinha et al. 2013, Rodrigues et al. 2014, 2019, Laaß 2015, Balanoff et al. 2016, Benoit et al. 2016, 2017a, b, Araújo et al. 2017, 2018, Laaß & Kaestner 2017, Laaß et al. 2017, Pavanatto et al. 2019, Oliveira et al. 2019, Hoffmann et al. 2019). Now it is possible to reconstruct three-dimensional models of the endocranial cavities non-destructively, different from previous approaches (*i.e.,* natural and artificial endocasts), with precise modeling of the impression of the soft tissues. Despite some limitations of the method (see Rodrigues et

al. 2014), the new efforts have been changing the way we understand the paleoneurological evolution of mammals and their precursors, the non-mammaliaform cynodonts (Benoit et al. 2016, Rowe 2017).

Riograndia guaibensis Bonaparte, Ferigolo, & Ribeiro 2001 is a small cynodont of the clade Ictidosauria from the Upper Triassic (Norian) of southern Brazil (Bonaparte et al. 2001, Martinelli & Rougier 2007). Its phylogenetic position close to the Mammaliaformes (Liu & Olsen 2010) makes this species important to understand the evolution of mammalian features. The morphology of the skull and post-cranial bones of *R. guaibensis* have been studied (Bonaparte et al. 2001, Soares et al. 2011, Guignard et al. 2019), and recently the brain endocast morphology of

one specimen (UFRGS-PV-596-T) was analyzed by Rodrigues et al. (2019). As mentioned above, although a significant advance has been achieved in the last years, most of our knowledge of non-mammaliaform therapsids is based on the study of one specimen of each taxon, with some exceptions (see Pavanatto et al. 2019 and Hoffmann et al. 2019 for a discussion on intraspecific variation). In most cases, this is a limitation of our science, and thus, the information on the intraspecific/ontogenetic variation is restricted until new specimens are discovered.

In this study, we accessed the information from the brain endocast of an additional specimen referred to *R. guaibensis*, contributing to the neuroanatomical knowledge of Late Triassic non-mammaliaform cynodonts.

MATERIALS AND METHODS

The analyzed specimen is housed at the Paleontology Section of the Museu de Ciências Naturais (MCN), Secretaria do Meio Ambiente e Infraestrutura (SEMA-RS) under the collection number MCN-PV 10348. The specimen was collected from the Linha São Luiz site, Faxinal do Soturno, Rio Grande do Sul, Brazil. It comes from the *Riograndia* Assemblage Zone of the Candelária Sequence, Santa Maria Supersequence (Soares et al. 2011, Horn et al. 2014, Schultz et al. 2020). This site has been revealed several fossils since the end of the 1990 decade, mainly of small vertebrates, such as non-mammaliaform cynodonts, procolophonids, lepidosauromorphs (basal forms and sphenodontians), and dinosaurs (see Bonaparte et al. 2010 and Soares et al. 2011 for a review). Recently, the fossil-containing levels of this site were dated using $^{206}Pb/^{238}U$, revealing

a maximum age of deposition of 225.42 ± 0.37 million years (Langer et al. 2018).

MCN-PV 10348 was scanned with a µCT scan Skyscan™ 1173 in the Laboratório de Sedimentologia e Petrologia of the Pontifícia Universidade Católica do Rio Grande do Sul (PUCRS), Porto Alegre, Brazil. It was used 80 kV and 100 µA, and 1042 slices with a voxel size of 19.45 µm were obtained. The slices were analyzed with Mimics, and the regions of interest were manually segmented using a WACOM Cintiq 21UX tablet to generate 3D-models. The resulting 3D-models were rendered using Design Spark Mechanical 2.0. As the ventral and anterior regions of the endocranial cavity of non-mammaliaform cynodonts are usually not ossified, both regions are delimited artificially (see Pavanatto et al. 2019). The posteriormost region of the brain was not possible to be reconstructed confidently due to the fragmentation of the specimen.

For the estimate of body mass (BM) we employed the equation of Luo et al. (2001) [BM = $10^{(-3.83+3.68 \times \log(SL))}$] (SL: skull length). To calculate the encephalization quotients (EQs), we followed the protocol of Benoit et al. (2017a,b). They used three different EQs: Jerison (1973) [EQ = $BV/(0.12 \times BM^{0.67})$], Manger (2006) [EQ = $BV/0.0535 \times BM^{0.7294}$], and Hurlburt et al. (2013) [EQ = $BV/0.0155 \times BM^{0.553}$], in which BV is the brain volume and BM is the body mass. More details about EQs are available in Benoit et al. (2017a). We also employed Eisenberg (1981) [EQ = $BV/0.0553 \times BM^{0.74}$] to compare with previous interpretations. The endocranial space of non-mammalian therapsids was probably not fully occupied by the brain. Hence, before calculating the encephalization quotients, we converted the endocranial volume into brain volume, following Benoit et al. (2017a): brain volume in cm³ (or brain mass in g) = $10^{0.7828 (\log[\text{endocast volume in cm3}]) - 0.1318}$. This methodology was also applied to the specimen

UFRGS-PV-596-T following the data provided by Rodrigues et al. (2019).

Institutional abbreviations — **MCN-PV,** Paleontological Collection of the, Museu de Ciências Naturais, Secretaria do Meio Ambiente e Infraestrutura, Porto Alegre, RS, Brazil. **UFRGS-PV**, Paleovertebrate Collection, Universidade Federal do Rio Grande do Sul, Porto Alegre, RS, Brazil.

RESULTS

Brain endocast morphology

The specimen MCN-PV 10348 is a cranium, with the anteriormost tip of the snout broken off (Fig. 1a$_1$, b$_1$). The zygomatic arches are also missing, and the posterior region of the cranium is damaged, including part of the basicranium and the lateral wall of the braincase (Fig. 1a$_1$, b$_1$). The specimen preserves seven left upper postcanines (being the four last better preserved) and left two fragmented incisors (I2? and I3?) (Fig. 1a-c). The postcanine series shows imbricated crows, which are 'blade-like' and composed of sharp and aligned cuspules (Fig. 1a-c) (see Bonaparte et al. 2001). The anatomy of the bones and teeth is consistent with the type and other specimens referred to *Riograndia guaibensis* (Bonaparte et al. 2001, Soares et al. 2011), and their description is out of the scope of this contribution.

The endocranial cavity has no ossified anteroventral limits like in other non-mammaliaform therapsids (Hopson 1979, Rowe et al. 2011, Rodrigues et al. 2014), which exhibit a wide orbital vacuity (Fig. 1a$_2$, c). Regarding the roof of the endocranial cavity, there is an anteroposteriorly elongated concavity on the ventral surface of each parietal, which is transversally concave, separated by a midline ridge (Fig. 1e). These concavities represent the impression of the cerebral hemispheres. As typical for non-mammaliaform synapsids

(Rowe et al. 2011), there is no cribriform plate separating the brain cavity from the nasal cavity. However, there is a transversal ridge on the ventral surface of the frontals delimiting both endocranial regions (Fig. 1e). Also, there is an anteroposteriorly elongated ridge that separates both olfactory bulbs (Fig. 1e). The bones that encapsulate the hindbrain are damaged.

The brain endocast of MCN-PV 10348 was virtually reconstructed, and it was possible to access the morphology of the olfactory bulbs and tracts, forebrain, midbrain, and part of the hindbrain (Fig. 1f$_1$-f$_4$). However, the hindbrain is not confidently reconstructed because of the preservation of the specimen. Unossified zone and pineal body are absent in the brain endocast of *R. guaibensis,* as previously mentioned (Rodrigues et al. 2019).

The brain endocast occupies a large part of the endocranial space (Fig. 1a$_1$, b$_1$, d), measuring 18 mm in length and 7.3 mm in height (based on parameters proposed by Rodrigues et al. 2019) and a volume of 0.4070 cm^3. The anteriormost region of the brain endocast of MCN-PV 10348 shows the cast of the olfactory bulbs, encapsulated dorsally by the frontals. The bulbs are oval-shaped, and are 4.5 mm in length (25% of brain endocast length) and 2.5 mm in width (Fig. 1f). The dorsal profile of the bulbs is anteroposteriorly convex, (Fig. 1f$_3$-f$_4$). They are connected to the forebrain by a short olfactory tract, which forms a constriction between the bulbs and the cerebral hemispheres, but not forming a circular fissure (Fig. 1f$_1$).

MCN-PV 10348 has well-marked cerebral hemispheres on the dorsal surface of the brain endocast, which are separated by the median sulcus (Fig. 1f$_1$). They are 7 mm in length and 2 mm in width. The posteriormost region of the cerebral hemispheres has the same wide, approximately as the olfactory bulbs.
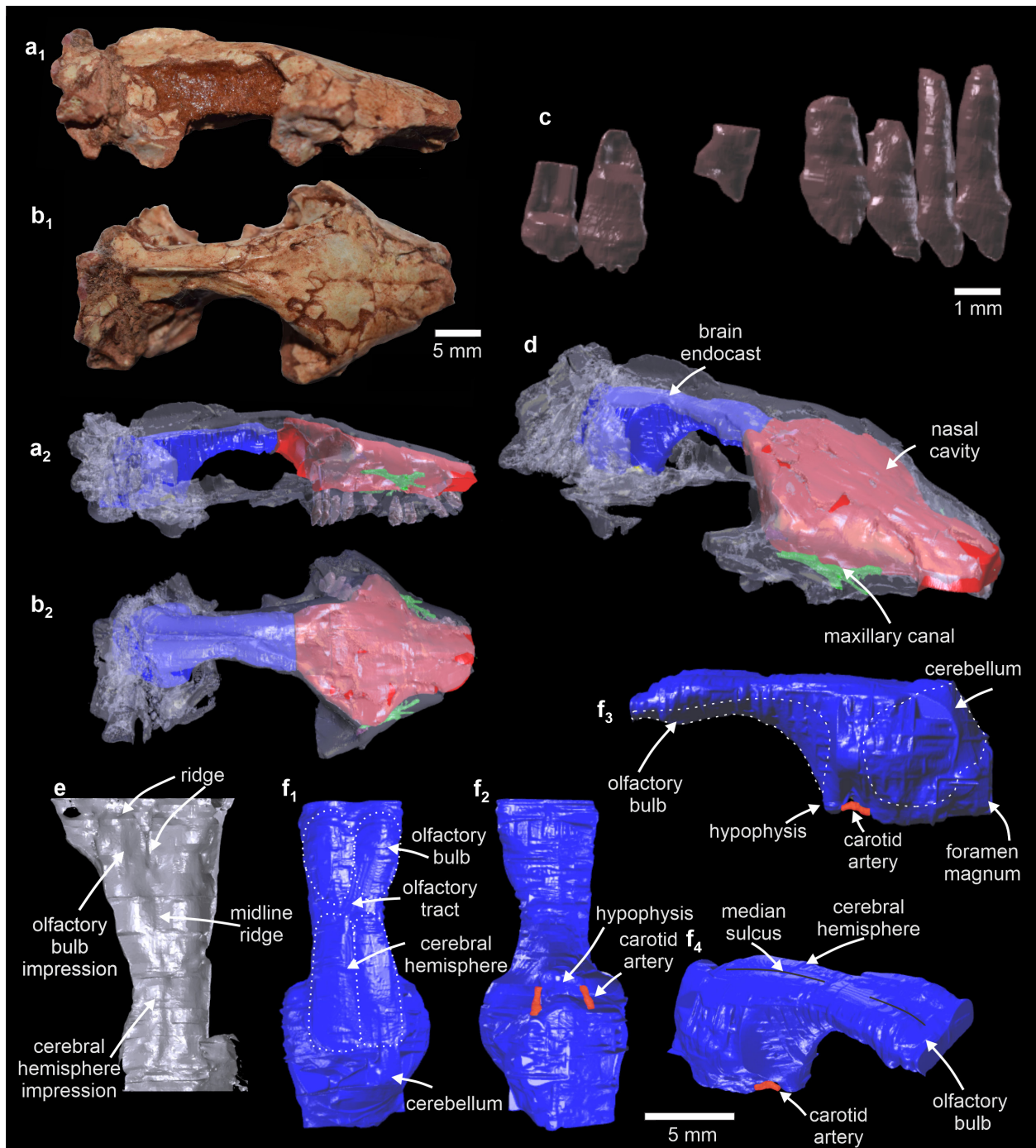
Figure 1. Cranium (MCN-PV 10348) and three-dimensional reconstructions of the endocranial cavities of *Riograndia guaibensis* from the Upper Triassic of southern Brazil. a_1-b_1, photographs of the cranium in lateral and dorsal views, respectively; c, three-dimensional reconstructions of the left postcanines, in labial view; a_2-b_2, d, translucent reconstructions of the cranium showing the endocranial cavities in lateral, dorsal, lateral oblique (slightly enlarged relative to the other two views) views, respectively; e, three-dimensional reconstruction of the cranial roof (frontal and parietal) in ventral view; f_1-f_4, brain endocast in dorsal, ventral, lateral, and lateral oblique views, respectively. Dashed areas on the endocast in lateral view (f_3) indicate the areas artificially delimited (ventral region) and areas in which the endocranial surface was not properly preserved to analyze the impression of soft tissues.

Ventrally, the endocast of MCN-PV 10348 shows a rounded cast of the hypophysis (1.54 mm x 1.97 mm) (Fig. 1f$_2$). Laterally to the hypophyseal cast, a short canal likely corresponds to the impression of the internal carotid artery (Fig. 1f$_2$-f$_4$). The region of the cerebellum is wider (8.5 mm in width) than the cerebral hemispheres, as in other non-mammaliaform cynodonts (*e.g.*, Rowe et al. 2011). This area, and other regions of the hindbrain, as the paraflocculus or the dorsal region of the cerebellum, cannot be described confidently due to the preservation of the specimen.

Encephalization quotients

A portion of the 3D surface of the brain endocast of MCN-PV 10348 was not possible to be confidently reconstructed to analyze its morphology, but an estimate of the endocranial volume was calculated (approximately 0.4070 cm^3) and converted into brain volume (0.3653 cm^3). With a cranium length of at least 40 mm (note that this measurement is estimated because the anteriormost tip of the snout is lacking), the body mass of MCN-PV 10348 is estimated in 114.8 g. With this data and the estimated volume of the brain volume, the EQs are 0.13 (Jerison 1973), 0.20 (Eisenberg 1981), 0.21 (Manger 2006), and 1.71 (Hurlburt et al. 2013). The results for the specimen UFRGS-PV-596-T using the data provided by Rodrigues et al. (2019) (endocranial volume without filling the space occupied by the interorbital vacuity during the segmentation= 0.4042 cm^3) are: brain volume, 0.3632 cm^3; body mass, 71.15 g; EQs: 0.17 (Jerison 1973), 0.28 (Eisenberg 1981), 0.30 (Manger 2006), and 2.21 (Hurlburt et al. 2013).

DISCUSSION AND FINAL REMARKS

The general morphology of the brain endocast of MCN-PV 10348 is very similar to that of UFRGS-PV-596-T, studied by Rodrigues et al. (2019). However, in the endocast analyzed by them, the sulcus dividing the cerebral hemispheres and well-defined olfactory bulbs are not clearly visible. That reconstruction exhibits a single concavity in the internal surface of the frontal and parietal bones, without a bony median ridge (although the authors interpreted that the real brain could have this division and not the plesiomorphic pattern of therapsids). Based on the 3D reconstruction of the endocranial cavity of MCN-PV 10348 here presented, these traits are present and, consequently, recognized for *R. guaibensis*. A conspicuous median sulcus on the dorsal surface of the brain endocast has been described for probainognathians in which the brain endocast morphology is known (Quiroga 1979, 1980, 1984, Rodrigues et al. 2014). Conversely, non-eucynodont cynodonts (*e.g.*, *Thrinaxodon*, Jerison 1973, Hopson 1979, Bird 2019: Fig. 2; *Galeasaurus*, Pusch et al. 2019) and gomphodonts (*e.g.*, Pavanatto et al. 2019, Hoffmann et al. 2019) do not have this condition. In cynodonts, the marked division of the cerebral hemispheres and well-defined olfactory bulbs are thus evident in species phylogenetically closer to Mammaliaformes, which illustrate the increase of encephalization during the synapsid evolution (*e.g.*, Rowe et al. 2011, Rodrigues et al. 2014). The cerebral hemispheres are anteroposteriorly oriented and have approximately the same width as the olfactory bulbs, slightly different from the schematic representation presented by Rodrigues et al. (2019), in which the hemispheres are posteriorly divergent, and are wider than the olfactory bulbs.

The encephalization quotients were calculated for MCN-PV 10348, revealing lower values than those obtained for the specimen UFRGS-PV-596-T assigned to *R. guaibensis*, and similar to *Brasilodon quadrangularis* and other non-mammaliaform cynodonts (see Rodrigues et al. 2014 and Benoit et al. 2017a; Table 1). Non-mammaliaform cynodonts have lower EQs than mammaliaforms, such as *Morganucodon* and *Hadrocodium* (Benoit et al. 2017a; Table 1), documenting a pulse of encephalization during the latest Triassic/early Jurassic (Rowe et al. 2011).

In sum, the endocranial morphology of MCN-PV 10348 demonstrates that *R. guaibensis* exhibits the same pattern shared by non-mammaliaform probainognathians. The specimen analyzed by Rodrigues et al. (2019) is approximately 35 mm in length. In contrast, the specimen studied here is slightly larger, which likely represents an advanced ontogenetic stage than the former one. Hence, the variability of the presence/absence of such traits and the EQs in both specimens may be correlated with the intraspecific variation of this cynodont, or alternatively, to the preservation of each specimen.

Acknowledgments

REFERENCES

ARAÚJO R, FERNANDEZ V, POLCYN MJ, FRÖBISCH J & MARTINS RMS. 2017. Aspects of gorgonopsian paleobiology and evolution: insights from the basicranium, occiput, osseous labyrinth, vasculature, and neuroanatomy. PeerJ: e3119.

ARAÚJO R, FERNANDEZ V, RABBITT RD, EKDALE EG, ANTUNES MT, CASTANHINHA R, FRÖBISCH J & MARTINS RMS. 2018. *Endothiodon* cf. *bathystoma* (Synapsida: Dicynodontia) bony labyrinth anatomy, variation, and body mass estimates. PLoS ONE 13: e0189883.

BALANOFF AM ET AL. 2016. Best practices for digitally constructing endocranial casts: examples from birds and their dinosaurian relatives. J Anat 229: 173-190.

BENOIT J, MANGER PR & RUBIDGE BS. 2016. Palaeoneurological clues to the evolution of defining mammalian soft tissue traits. Sci Rep 6: 25604.

BENOIT J, FERNANDEZ V, MANGER PR & RUBIDGE BS. 2017a. Endocranial casts of pre-mammalian therapsids reveal an unexpected neurological diversity at the deep evolutionary root of mammals. Brain Behav Evol 90: 311-333.

BENOIT J, MANGER PR, NORTON L, FERNANDEZ V & RUBIDGE BS. 2017b. Synchrotron scanning reveals the palaeoneurology of the head-butting *Moschops capensis* (Therapsida, Dinocephalia). PeerJ 5: e3496.

BIRD CM. 2019. Patterns in palaeontology: digitally peering inside fossil skulls. Palaeontology Online 9: 1-7.

BONAPARTE JF, FERIGOLO J & RIBEIRO AM. 2001. A primitive Late Triassic 'ictidosaur' from Rio Grande do Sul, Brazil. Palaeontology 44: 623-635.

BONAPARTE JF, SCHULTZ CL, SOARES MB & MARTINELLI AG. 2010. La fauna local de Faxinal do Soturno, Triásico Tardío de Rio Grande do Sul, Brasil. Rev Bras Paleontolog 13: 233-246.

CASTANHINHA R, ARAÚJO R, JÚNIOR CL, ANGIELCZYK KD, MARTINS GG, MARTINS RMS, CHAUOUIYA C, BECKMANN F & WILDE F. 2013. Bringing dicynodonts back to life: paleobiology and anatomy of a new emydopoid genus from the Upper Permian of Mozambique. PLoS ONE 8: e80974.

EISENBERG JF. 1981. The Mammalian Radiations: An Analysis of Trends in Evolution, Adaptation, and Behavior. Chicago: University Chicago Press, 610 p.

GUIGNARD ML, MARTINELLI AG & SOARES MB. 2019. Postcranial anatomy of *Riograndia guaibensis* (Cynodontia: Ictidosauria). Geobios 53: 9-21.

HOPSON JA. 1979. Paleoneurology. In: Gans C, Northcutt RG & Ulinski PC (Eds), Biology of the Reptilia, AP, New York, p. 39-146.

HOFFMANN CA, RODRIGUES PG, SOARES MB & ANDRADE MB. 2019. Brain endocast of two non-mammaliaform cynodonts from southern Brazil: an ontogenetic and evolutionary approach. Hist Biol. Online first.

HORN BLD, MELO TM, SCHULTZ CL, PHILIPP RP, KLOSS HP & GOLDBERG K. 2014. A new third-order sequence stratigraphic framework applied to the Triassic of the Paraná Basin, Rio Grande do Sul, Brazil, based on structural, stratigraphic and paleontological data. J S Am Earth Sciences 55: 123-132.

HURLBURT GR, RIDGELY RC & WITMER LM. 2013. Relative size of brain and cerebrum in tyrannosaurid dinosaurs: An analysis using brain endocast quantitative relationships in extant alligators. In Parrish JM, Molnar RE, Currie PJ & Koppelhus EB (Eds), Tyrannosaurid paleobiology. Blooming, Indiana University Press, p. 135-154.

JERISON HJ. 1973. Evolution of the brain and intelligence. AP, New York, 482 p.

LAAß M. 2015. virtual reconstruction and description of the cranial endocast of *Pristerodon mackayi* (Therapsida, Anomodontia). J Morphol 276: 1089-1099.

LAAß M & KAESTNER A. 2017. Evidence for convergent evolution of a neocortex-like structure in a late Permian therapsid. J Morphol 278: 1033-1057.

LAAß M, SCHILLINGER B & KAESTNER A. 2017. What did the "unossified zone" of the non-mammalian therapsid braincase house ?. J Morphol 278: 1020-1032.

LANGER MC, RAMEZANI J & DA-ROSA AAS. 2018. U-Pb age constraints on dinosaur rise from south Brazil. Gondwana Res 57: 133-140

LIU J & OLSEN P. 2010. The phylogenetic relationships of Eucynodontia (Amniota: Synapsida). J Mamm Evol 17: 151-176.

LUO ZX, CROMPTON AW & SUN AL. 2001. A new mammaliaform from the Early Jurassic and evolution of mammalian characteristics. Science 292: 1535-1540.

MANGER PR. 2006. An examination of cetacean brain structure with a novel hypothesis correlating thermogenesis to the evolution of a big brain. Biol Rev 81: 293-338.

MARTINELLI AG & ROUGIER GW. 2007. On *Chaliminia musteloides* Bonaparte (Cynodontia, Tritheledontidae) and the phylogeny of the Ictidosauria. J Vertebr Paleontol 27: 442-460.

OLIVEIRA DS, KERBER L & PINHEIRO F. 2020. Endocranial morphology of the Brazilian Permian dicynodont *Rastodon procurvidens* (Therapsida: Anomodontia). J Anat 236: 384-397.

PAVANATTO AEB, KERBER L & DIAS-DA-SILVA S. 2019. Virtual reconstruction of cranial endocasts of traversodontid cynodonts (Eucynodontia: Gomphodontia) from the upper Triassic of Southern Brazil. J Morphol 280: 1267-1281.

PUSCH LC, KAMMERER CF & FRÖBISCH J. 2019. Cranial anatomy of the early cynodont *Galesaurus planiceps* and the origin of mammalian endocranial characters. J Anat 234: 592-621.

QUIROGA JC. 1979. The brain of two mammal-like reptiles (Cynodontia-Therapsida). J Hirnforsch 20: 351-359.

QUIROGA JC. 1980. Further studies on cynodont endocasts (Reptilia-Therapsida). Z Mikrosk Anat Forsc 94: 580-592.

QUIROGA JC. 1984. The endocranial cast of the advanced mammal-like reptile *Therioherpeton cargnini* (Therapsida-Cynodontia) form the Middle Triassic of Brazil. J Hirnforschu 25: 285-290.

RODRIGUES PG, MARTINELLI AG, SCHULTZ CL, CORFE IJ, GILL PG, SOARES MB & RAYFIELD EJ. 2019. Digital cranial endocast of *Riograndia guaibensis* (Late Triassic, Brazil) sheds light on the evolution of the brain in non-mammalian cynodonts. Hist Biol 31: 1195-1212.

RODRIGUES PG, RUF I & SCHULTZ CL. 2014. Study of a digital cranial endocast of the non-mammaliaform cynodont *Brasilitherium riograndensis* (Later Triassic, Brazil) and its relevance to the evolution of the mammalian brain. Paläontol Z 88: 329-352.

ROWE TB. 2017. The emergence of mammals. In: Kaas J (Ed), Evolution of Nervous Systems. Elsevier, Oxford, 2: 1-52.

ROWE TB, MACRINI TE & LUO ZX. 2011. Fossil evidence on origin of the mammalian brain. Science 332: 955-957.

SCHULTZ CL, MARTINELLI AG, SOARES MB, PINHEIRO FL, KERBER L, HORN LDB, PRETTO FA, MÜLLER RT & MELO T. 2020. Triassic faunal successions of the Paraná Basin, southern Brazil. J S Am Earth Sciences 104: 102846.

SOARES MB, SCHULTZ CL & HORN BLD. 2011. New information on *Riograndia guaibensis* Bonaparte, Ferigolo & Ribeiro, 2001 (Eucynodontia, Tritheledontidae) from the Late Triassic of southern Brazil: anatomical and biostratigraphic implications. An Acad Bras Cienc 83: 329-354.

LEONARDO KERBER[1,2,3]
https://orcid.org/0000-0001-8139-1493

JOSÉ DARIVAL FERREIRA[3]
https://orcid.org/0000-0002-2779-6120

PEDRO HENRIQUE M. FONSECA[4]
https://orcid.org/0000-0001-7721-9818

ARYMATHEIA FRANCO[3]
https://orcid.org/0000-0001-7341-259X

AGUSTÍN G. MARTINELLI[5]
https://orcid.org/0000-0003-4489-0888

MARINA BENTO SOARES[4,6]
http://orcid.org/0000-0002-8393-2406

ANA MARIA RIBEIRO[4,7]
https://orcid.org/0000-0003-4167-8558

[1]Universidade Federal de Santa Maria, Centro de Apoio à Pesquisa Paleontológica, Rua Maximiliano Vizzotto, 598, 97230-000 São João do Polêsine, RS, Brazil

[2]Museu Paraense Emílio Goeldi, Coordenação de Ciências da Terra e Ecologia, Av. Perimetral, 1901, 66077-830 Belém, PA, Brazil

[3]Universidade Federal de Santa Maria, Programa de Pós-Graduação em Biodiversidade Animal, Av. Roraima 1000, 97105-900 Santa Maria, RS, Brazil

[4]Universidade Federal do Rio Grande do Sul, Programa de Pós-Graduação em Geociências, Av. Bento Gonçalves, 9500, 91501-970 Porto Alegre, RS, Brazil

[5]Museo Argentino de Ciencias Naturales 'Bernardino Rivadavia', CONICET-Sección Paleontología de Vertebrados, Av. Ángel Gallardo, 470, C1405 DJR, Buenos Aires, Argentina

[6]Universidade Federal do Rio de Janeiro, Museu Nacional, Departamento de Geologia e Paleontologia, Quinta da Boa Vista, São Cristóvão, 20940-040 Rio de Janeiro, RJ, Brazil

[7]Secretaria do Meio Ambiente e Infraestrutura, Museu de Ciências Naturais, Seção de Paleontologia, Av. Salvador França, 1427, 90690-000 Porto Alegre, RS, Brazil

Correspondence to: **Leonardo Kerber**
E-mail: leonardokerber@gmail.com

Author contributions

LK, JDF, PHMF, AF, AGM, MBS and AMR conducted the research. The 3D model was generated by LK. The manuscript was written by LK, JDF, PHMF, AF, AGM, MBS and AMR. The figure was prepared by LK. JDF performed the quantitative analysis. All authors approved the submission of this work.